

## Magnetic properties of GaAs-Fe<sub>3</sub>Si core-shell nanowires—A comparison of ensemble and single nanowire investigation

Maria Hilse, Bernd Jenichen, and Jens Herfort

Citation: *AIP Advances* **7**, 056305 (2017);

View online: <https://doi.org/10.1063/1.4973748>

View Table of Contents: <http://aip.scitation.org/toc/adv/7/5>

Published by the [American Institute of Physics](#)

---

### Articles you may be interested in

[Structure and properties of sintered MM-Fe-B magnets](#)

*AIP Advances* **7**, 056215 (2017); 10.1063/1.4973603

[Magnetic properties of Nd\(Fe<sub>1-x</sub>Co<sub>x</sub>\)<sub>10.5</sub>M<sub>1.5</sub> \(M=Mo and V\) and their nitrides](#)

*AIP Advances* **7**, 056202 (2016); 10.1063/1.4973207

[The magnetic properties of MMCo<sub>5</sub> \(MM=Mischmetal\) nanoflakes prepared by multistep \(three steps\) surfactant-assisted ball milling](#)

*AIP Advances* **7**, 056203 (2016); 10.1063/1.4973395

[Patterning of two-dimensional electron systems in SrTiO<sub>3</sub> based heterostructures using a CeO<sub>2</sub> template](#)

*AIP Advances* **7**, 056410 (2017); 10.1063/1.4973696

[Magnetic properties of Sm-Fe-N bulk magnets produced from Cu-plated Sm-Fe-N powder](#)

*AIP Advances* **7**, 056204 (2016); 10.1063/1.4973396

[Magnetic stripes and holes: Complex domain patterns in perforated films with weak perpendicular anisotropy](#)

*AIP Advances* **7**, 056303 (2016); 10.1063/1.4973284

---

# HAVE YOU HEARD?

Employers hiring scientists and engineers trust

**PHYSICS TODAY | JOBS**

[www.physicstoday.org/jobs](http://www.physicstoday.org/jobs)



# Magnetic properties of GaAs-Fe<sub>3</sub>Si core-shell nanowires—A comparison of ensemble and single nanowire investigation

Maria Hilse,<sup>a</sup> Bernd Jenichen, and Jens Herfort  
*Paul-Drude-Institute Berlin, Hausvogteiplatz 5-7, 10117 Berlin, Germany*

(Presented 3 November 2016; received 19 September 2016; accepted 20 October 2016; published online 4 January 2017)

On the basis of semiconductor-ferromagnet GaAs-Fe<sub>3</sub>Si core-shell nanowires (Nws) we compare the facilities of magnetic Nw ensemble measurements by superconducting quantum interference device magnetometry versus investigations on single Nws by magnetic force microscopy and computational micromagnetic modeling. Where a careful analysis of ensemble measurements backed up by transmission electron microscopy gave no insights on the properties of the Nw shells, single Nw investigation turned out to be absolutely essential. © 2017 Author(s). All article content, except where otherwise noted, is licensed under a Creative Commons Attribution (CC BY) license (<http://creativecommons.org/licenses/by/4.0/>). [<http://dx.doi.org/10.1063/1.4973748>]

## I. INTRODUCTION

In the last years, semiconductor-ferromagnet core-shell nanowires (SFCSNws) attract quite a lot of attention as they are regarded as promising candidates for a number of forward-looking devices in the field of spintronics and magnetic recording.<sup>1–12</sup> To fabricate SFCSNws, commonly first semiconductor Nws are fabricated by epitaxial methods such as molecular beam epitaxy or metal oxide chemical vapor deposition and are in a second growth step coated with the ferromagnetic material. Thereby the magnetic material does not necessarily stick to the Nw shells exclusively. It rather grows where the material flux reaches the sample. This is due to the quite low growth temperatures that are used and the therefore high sticking coefficient almost everywhere on the sample. Thus, as-grown samples always comprise SFCSNws as well as a parasitic ferromagnetic layer between the Nws.

For the above mentioned device fabrication, an appropriate magnetic characterization of such SFCSNws is mandatory. This can be done either by ensemble measurement techniques or single Nw investigation methods. Ensemble measurements have the advantage that they give quite good statistics by averaging over a large number of Nws on a sample but as a disadvantage they contain also contributions from magnetic material on the sample that does not belong to the Nw shells, such as the parasitic ferromagnetic layer between the Nws. Thus, the insight of ensemble measurements on the Nws themselves that were reported recently by using superconducting quantum interference device magnetometry (SQUID), small angle neutron scattering and ferromagnetic resonance techniques are quite equivocal.<sup>1–7</sup> Single Nw magnetic investigation on the other hand gives precise information about only the selected structure (one Nw shell) but thus it reflects only the information obtained from one single event of measurement (from one Nw). To draw conclusions from such measurements over all other Nws is hence quite limited. To investigate single Nws, electrical measurements of the magnetoresistance, magnetic force microscopy (MFM) and nanoSQUID techniques were used so far in literature.<sup>5,8–12</sup>

---

<sup>a</sup>Electronic mail: [dr.maria.hilse@t-online.de](mailto:dr.maria.hilse@t-online.de)

In this study, we give an overview and compare the capability of the commonly used magnetic ensemble and single Nw magnetic characterization on the basis of GaAs-Fe<sub>3</sub>Si core-shell Nws. Details on the growth and structural properties of these Nws can be found elsewhere.<sup>5,13–15</sup> In the first part of this article, we report on the ensemble measurements which were carried out using SQUID at room temperature (RT). In the second part, we present magnetic single Nw investigation. For this purpose, we used MFM at RT and numerical micromagnetic modeling by the finite element simulation tool Nmag.<sup>16</sup>

## II. ENSEMBLE NW CHARACTERIZATION

As mentioned above, the as-grown SFCSNw samples comprise two main magnetic contributions; first the Nw shells and second an unintentionally grown planar magnetic layer between the Nws. Details on the growth can be found elsewhere.<sup>5</sup> Both contributions can be seen in the bright-field transmission electron micrograph (TEM) of GaAs-Fe<sub>3</sub>Si core-shell Nws in Fig. 1(a). The Nws are oriented along the out-of-plane [111] direction on a Si(111) substrate that is covered with a thin native oxide layer. The Fe<sub>3</sub>Si shell grows on the GaAs facets whereas the parasitic layer grows on top of the amorphous oxide. In the following these samples are referred to as sample configuration A. To distinguish later on in the ensemble measurements between a contribution from the Nw shells and a second from the parasitic layer, two additional sample configurations were prepared. After the

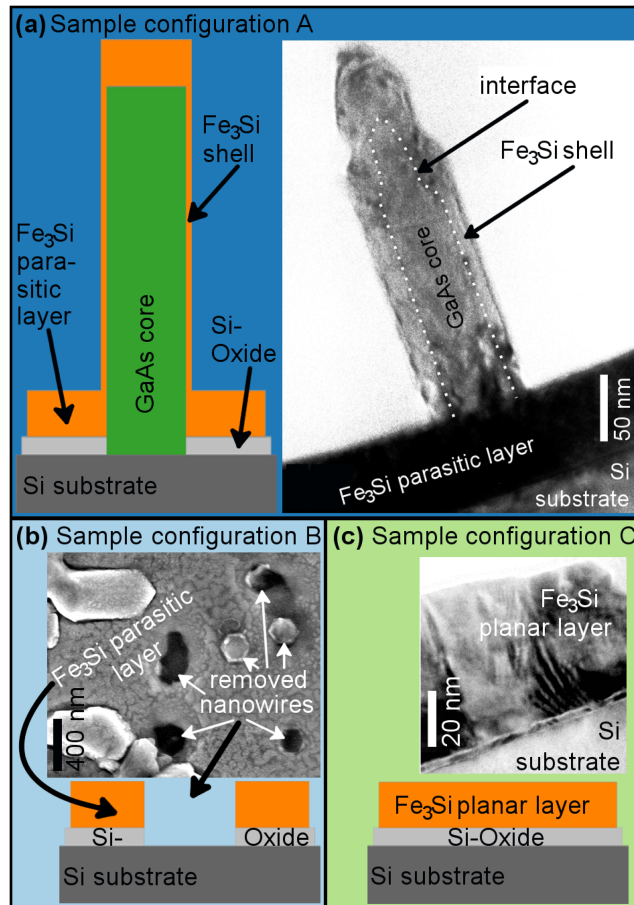


FIG. 1. Sketches and TEM/SEM images of the three sample configurations used for ensemble Nw characterization with a Fe<sub>3</sub>Si growth temperature of 200 °C. (a) TEM side view of sample A: an as-grown GaAs-Fe<sub>3</sub>Si core-shell Nw sample. (b) SEM top view of sample B: the as-grown sample A with removed Nws which are indicated by arrows. It contains the parasitic Fe<sub>3</sub>Si layer and with Fe<sub>3</sub>Si covered GaAs islands only. (c) TEM cross section of sample C: a planar Fe<sub>3</sub>Si film.

measurement of sample A, the Nws of this sample were removed. This was done in an ultrasonic bath and checked with scanning electron microscopy (SEM). The obtained sample now only consists of the parasitic  $\text{Fe}_3\text{Si}$  film and with  $\text{Fe}_3\text{Si}$  covered GaAs islands that typically grow as well during the self-assisted vapor-liquid-solid GaAs Nw growth mechanism. It is shown in Fig. 1(b) and represents sample configuration B. Finally an equally thick planar  $\text{Fe}_3\text{Si}$  layer was grown under identical conditions that were used for the core-shell Nw growth on the same substrate i.e., a Si(111) substrate covered with a thin native oxide layer. This is labeled sample configuration C and shown in Fig. 1(c).

Samples of all three configurations with  $\text{Fe}_3\text{Si}$  growth temperatures of 100, 200, 300, and 350 °C were measured with SQUID at RT. The external field was applied along the two major in-plane directions  $\langle 11\bar{2} \rangle$ , and  $\langle 1\bar{1}0 \rangle$ , and along the out-of-plane  $[111]$  direction, i.e. along the Nw axis. Exemplarily, the obtained  $M$ - $H$ -curves for samples A(100 °C), B(100 °C), and C(100 °C) i.e., samples A, B, and C with a  $\text{Fe}_3\text{Si}$  growth temperature of 100 °C measured along the out-of-plane  $[111]$  direction can be found in Figs. 2(b) and 2(b). Similar results are obtained for all sample configurations at higher  $\text{Fe}_3\text{Si}$  growth temperatures. In general, all samples show a very hard magnetic axis along the  $[111]$  direction with anisotropy fields of about 20 kOe, which lies in the typical range for  $\text{Fe}_3\text{Si}$ . A potential parallel magnetization of the SFCSNws, i.e. a spontaneous magnetization oriented along the  $[111]$  direction in addition to the in-plane magnetization of the parasitic layer would reduce the measured effective anisotropy field for sample A exclusively which was not observed. In the small field region in Fig. 2(b), a hysteresis is present for all sample configurations. This hysteresis may result from the SFCSNws. However, as samples B and C without Nws as well show a hysteresis, small sample tilts during the measurement may as well cause the observed hysteresis.

In the in-plane directions, as shown exemplarily for A(100 °C) in Fig. 2(c), magnetically isotropic behavior with almost identical anisotropy fields was found for all samples. An additional easy or hard axis contribution from the Nw shells exclusively for sample A was also not observed in these directions.

This leads to the suggestion that either the Nw shells possess as well as the parasitic layer an in-plane magnetization or the parasitic layer completely dominates the magnetic ensemble measurements. A mathematical estimation of the volume of ferromagnetic material gave an overall Nw shell

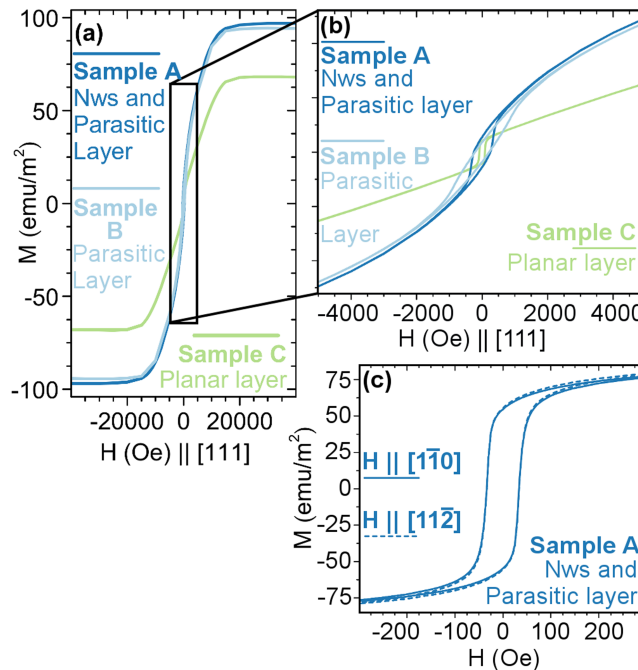


FIG. 2. (a) and (b): Magnetic moment of the samples A(100 °C), B(100 °C), and C(100 °C) over an external field parallel to the  $[111]$  direction. (a)  $M$ - $H$ -curves up to the high field region. (b) Hysteresis at small fields. (c) Magnetic moment dependence of sample A(100 °C) measured along the two in-plane directions  $\langle 1\bar{1}0 \rangle$  and  $\langle 11\bar{2} \rangle$ .

volume of only (0.5 - 12) % of the parasitic layer volume. Thus, the above suggestion of a dominating parasitic layer in the ensemble measurement is quite reasonable. However, after the presented ensemble measurement investigation of three different sample configurations by a such powerful tool as SQUID magnetometry it can be deduced that it is not possible to elucidate a discrete magnetic contribution from the Nw shells. Thus, ensemble measurements are not suited to investigate the magnetic texture of ferromagnetic Nw shells. For this purpose, an investigation of single Nws is indispensable.

More information on the magnetic ensemble investigation can be found in the [supplementary material](#).

### III. SINGLE NW CHARACTERIZATION

To investigate the magnetic properties of single Nws, we carried out MFM on Nws that were first removed from the as-grown sample configuration A via an ultrasonic bath in a solvent and then transferred to a second clean substrate. The obtained MFM phase maps combined with an image of the atomic force microscopy (AFM) topography of several Nws with a  $\text{Fe}_3\text{Si}$  growth temperature of 100 °C are presented in Figure 3. The observed MFM phase contrast differs significantly from the topological contrast. Nws were scanned at different angles. Thus the observed phase contrast is not an artifact of the needle movement. All Nws show a distinct and circular shaped dark end and opposite a similar bright end where magnetic forces act on the magnetic tip.

To convert the observed MFM phase contrast into a specific magnetization in the Nw shells, the magnetic field of the sample as well as the magnetic moment of the needle have to be calculated precisely.<sup>17</sup> In general, this is not possible but in a first and simple approximation of the tip's moment in the direction perpendicular to the sample, the observed phase shift is proportional to the first or second derivative of the sample's magnetic field in this direction.<sup>17</sup> Thus, the magnetic field of one Nw with a distinct magnetization needs to be calculated. This has been done with the numerical python based finite element micromagnetic simulation tool Nmag.<sup>16</sup> More details to this micromagnetic modeling can be found in the [supplementary material](#).

In magnetic nanotubes, there are only two stable magnetic configurations. These are first the parallel state with  $\vec{M} = (0, 0, M_S)$  and second the vortex state with  $\vec{M} = M_S \vec{e}_\varphi$ .<sup>18</sup> Whether the equilibrium orientation of the spontaneous magnetization will adapt the vortex or the parallel state depends on nanotube geometry, crystal anisotropy energies and saturation magnetization of the magnetic material.<sup>19,20</sup> As it is shown in Figures 4(a) and 4(b), the first and second derivative of the magnetic field  $H_x$  in the (y,z)-plane for these two magnetic states differ completely. Whereas the vortex state gives an opposing maximum and minimum of magnetic field along the z axis of the wire that is

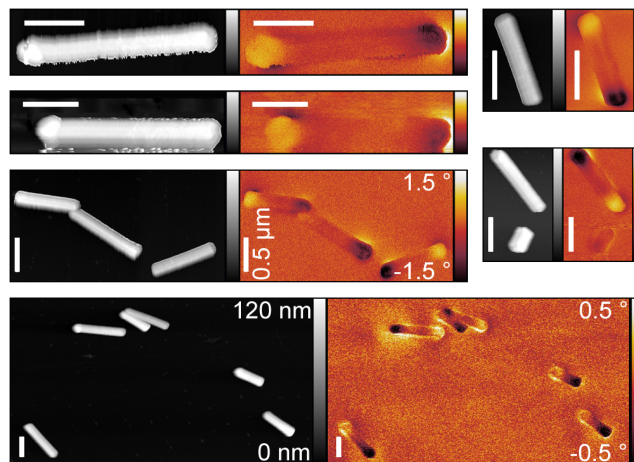


FIG. 3. AFM (black-white) and MFM maps of several Nws with a  $\text{Fe}_3\text{Si}$  growth temperature of 100 °C at a scale of 0.5  $\mu\text{m}$ . The height in the AFM images ranges between 0 and 120 nm, the phase shift of the MFM maps ranges between -1.5 and 1.5 ° except for the lower MFM image with a scale from -0.5 to 0.5 °.

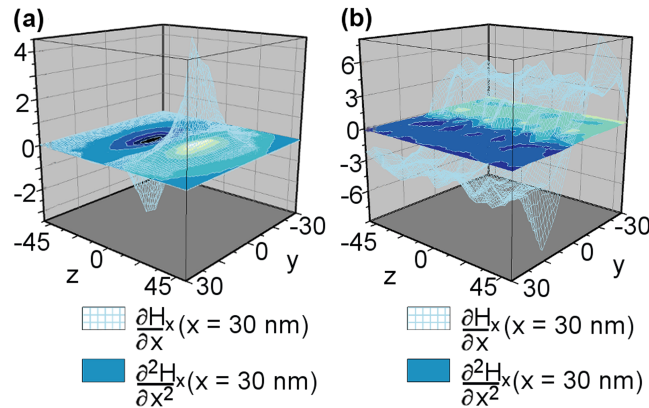


FIG. 4. Three-dimensional ( $y,z$ )-map of the first and second derivative of the magnetic field strength in  $x$ -direction of one Nw calculated by Nmag<sup>16</sup> in a distance of 30 nm over the wire in  $10^3 \text{ A}/(\text{nm}\cdot\text{m})$ , and  $10^3 \text{ A}/(\text{nm}^2\cdot\text{m})$ , respectively. (a) Nw with  $\vec{M} = (0, 0, M_S)$ . (b) Nw with  $\vec{M} = M_S \vec{e}_\varphi$ .

uniformly spread along the whole length of the tube, the parallel state leads to a significant magnetic field contribution at the ends of the tube only. Thus, the observed phase shift in MFM can be clearly attributed to a magnetization along the tube. Single Nw investigation hence revealed a spontaneous magnetic moment in the Nw shells that is oriented along the wire, i.e. along the out-of-plane direction of the as-grown samples. It is hence completely different from the moment's orientation obtained by the above discussed ensemble SQUID measurements. This evidences that the parasitic planar layer between the Nws dominates even in very carefully performed magnetic ensemble investigation.

#### IV. CONCLUSION

The ensemble magnetic measurements by SQUID magnetometry of GaAs-Fe<sub>3</sub>Si core-shell Nws were completely dominated by the extensive parasitic Fe<sub>3</sub>Si layer between the Nws. Thus, with such ensemble techniques it is not possible to draw any conclusions about the magnetic properties of the Fe<sub>3</sub>Si Nw shells. To gain insights about these properties, single Nw characterization is absolutely essential. In our study the single measurement technique showed for the SFCSNws in contrast to the ensemble investigation a magnetization along the wire. This is of general interest, as it applies to all the so far presented SFCSNws where a significant amount of magnetic material grows as well between the Nws and should be taken into account when analyzing ensemble magnetic measurements. Nevertheless, as side note, ensemble magnetic measurements are a powerful tool to investigate the magnetic properties of Nws in the case of a suppressed parasitic layer growth. This can be realized for example by increasing the Nw density and length such that the sample space between the Nws is shadowed by the Nws. However, such high Nw densities have not been demonstrated for SFCSNw growth so far.

#### SUPPLEMENTARY MATERIAL

See [supplementary material](#) for experimental details and additional characterization data can be found in the supplementary material.

#### ACKNOWLEDGMENTS

The authors thank Claudia Herrmann for technical assistance in maintaining the MBE and Mirko Heckert for recording the SQUID measurements. Furthermore the author thanks Konrad Hilse for assistance in information technology. This work has been funded by the Caroline von Humboldt program of Humboldt-University Berlin.

- <sup>1</sup> X. Yu, H. Wang, D. Pan, J. Zhao, J. Misuraca, S. von Molnár, and P. Xiong, "All zinc-blende GaAs/(Ga,Mn)As core-shell nanowires with ferromagnetic ordering," *Nano Lett.* **13**, 1572 (2013).
- <sup>2</sup> R. E. Pimpinella, D. Zhang, M. R. McCartney, D. J. Smith, K. L. Krycka, B. J. Kirby, B. J. O'Dowd, L. Sonderhouse, J. Leiner, X. Liu, M. Dobrowolska, and J. K. Furdyna, "Magnetic properties of GaAs/Fe core/shell nanowires," *Journal of Applied Physics* **113**, 17B520 (2013).
- <sup>3</sup> K. Tivakornsasithorn, R. E. Pimpinella, V. Nguyen, X. Liu, M. Dobrowolska, and J. K. Furdyna, "Magnetic anisotropy of GaAs/Fe/Au core-shell nanowires grown by MBE," *J. Vac. Sci. Technol. B* **30**, 02B115 (2012).
- <sup>4</sup> M. Hilse, Y. Takagaki, J. Herfort, M. Ramsteiner, C. Herrmann, S. Breuer, L. Geelhaar, and H. Riechert, "Ferromagnet-semiconductor nanowire coaxial heterostructures grown by molecular-beam epitaxy," *Appl. Phys. Lett.* **95**, 133126 (2009).
- <sup>5</sup> M. Hilse, J. Herfort, B. Jenichen, A. Trampert, M. Hanke, P. Schaaf, L. Geelhaar, and H. Riechert, "GaAs-Fe<sub>3</sub>Si core-shell nanowires: Nanobar magnets," *Nano letters* **13**, 6203–6209 (2013).
- <sup>6</sup> Y. Takagaki, J. Herfort, M. Hilse, L. Geelhaar, and H. Riechert, "Swingback in magnetization reversal in MnAs-GaAs coaxial nanowire heterostructures," *Journal of Physics: Condensed Matter* **23**, 1–9 (2011).
- <sup>7</sup> A. Rudolph, M. Soda, M. Kiessling, T. Wojtowicz, D. Schuh, W. Wegscheider, J. Zweck, C. Back, and E. Reiger, "Ferromagnetic GaAs/GaMnAs core-shell nanowires grown by molecular beam epitaxy," *Nano Lett.* **9**, 3860 (2009).
- <sup>8</sup> J. Liang, J. Wang, a. Paul, B. J. Cooley, D. W. Rench, N. S. Deltas, S. E. Mohny, R. Engel-Herbert, and N. Samarth, "Measurement and simulation of anisotropic magnetoresistance in single GaAs/MnAs core/shell nanowires," *Applied Physics Letters* **100**, 182402 (2012).
- <sup>9</sup> C. Butschkow, E. Reiger, A. Rudolph, S. Geißler, D. Neumaier, M. Soda, D. Schuh, G. Woltersdorf, W. Wegscheider, and D. Weiss, "Origin of negative magnetoresistance of GaAs/(Ga,Mn)As core-shell nanowires," *Physical Review B* **87**, 245303 (2013).
- <sup>10</sup> D. Ruffer, R. Huber, and P. Berberich, "Magnetic states of an individual Ni nanotube probed by anisotropic magnetoresistance," *Nanoscale* **4**, 4989 (2012).
- <sup>11</sup> D. P. Weber, D. Ruffer, A. Buchter, F. Xue, E. Russo-Averchi, R. Huber, P. Berberich, J. Arbiol, A. Fontcuberta I Morral, D. Grundler, and M. Poggio, "Cantilever magnetometry of individual Ni nanotubes," *Nano letters* **12**, 6139 (2012).
- <sup>12</sup> A. Buchter, J. Nagel, D. Ruffer, F. Xue, D. P. Weber, O. F. Kieler, T. Weimann, J. Kohlmann, A. B. Zorin, E. Russo-Averchi, R. Huber, P. Berberich, A. Fontcuberta i Morral, M. Kemmler, R. Kleiner, D. Koelle, D. Grundler, and M. Poggio, "Reversal mechanism of an individual Ni nanotube simultaneously studied by Torque and SQUID magnetometry," *Physical Review Letters* **111**, 067202 (2013).
- <sup>13</sup> B. Jenichen, M. Hilse, J. Herfort, and A. Trampert, "Real structure of lattice matched GaAs-Fe<sub>3</sub>Si core-shell nanowires," *J. Cryst. Growth* **410**, 1 (2015).
- <sup>14</sup> B. Jenichen, M. Hilse, J. Herfort, and A. Trampert, "Facetted growth of Fe<sub>3</sub>Si shells around GaAs nanowires on Si(111)," *J. Cryst. Growth* **427**, 21 (2015).
- <sup>15</sup> B. Jenichen, M. Hanke, M. Hilse, J. Herfort, A. Trampert, and S. C. Erwin, "Diffraction at GaAs/Fe<sub>3</sub>Si core/shell nanowires: the formation of nanofacets," *AIP Advances* **6**, 055108 (2016).
- <sup>16</sup> T. Fischbacher, M. Franchin, G. Bordignon, and H. Fangohr, "A systematic approach to multiphysics extensions of finite-element-based micromagnetic simulations: Nmag," *IEEE Transactions on Magnetics* **43**, 2896–2898 (2007).
- <sup>17</sup> NT-MDT, Magnetic Force Microscopy : Quantitative Results Treatment, Internet, 2014.
- <sup>18</sup> P. Landeros, J. Escrig, D. Altbir, D. Laroze, J. dAlbuquerque e Castro, and P. Vargas, "Scaling relations for magnetic nanoparticles," *Physical Review B* **71**, 094435 (2005).
- <sup>19</sup> J. Escrig, P. Landeros, D. Altbir, E. Vogel, and P. Vargas, "Phase diagrams of magnetic nanotubes," *J. Magn. Magn. Mater* **308**, 233 (2007).
- <sup>20</sup> J. Escrig, P. Landeros, D. Altbir, and E. Vogel, "Effect of anisotropy in magnetic nanotubes," *J. Magn. Magn. Mater* **310**, 2448 (2007).